Diffusion and Defect Reactions
in Isotopically Controlled Semiconductors

Hartmut Bracht

Universität Münster, Institut für Materialphysik, Wilhelm-Klemm-Str. 10,
D-48149 Münster, Germany,

E-Mail: bracht@uni-muenster.de

Abstract. Point defects in semiconductors play a decisive role for the functionality of semiconductors. A detailed, quantitative understanding of diffusion and defect reactions of dopants is required for advanced modelling of modern nanometer size electronic devices. With isotope heterostructures which consist of epitaxial layers of isotopically pure and deliberately mixed stable isotopes, we have studied the simultaneous self- and dopant diffusion in several major semiconductors such as silicon and germanium. Detailed analysis of the simultaneous diffusion of self- and dopant atoms in Si and Ge yields information about the ionization levels of native defects and about dopant-defect interactions in Si and Ge. The results of these diffusion studies are highlighted in this work.

1 Introduction

The understanding of defect reactions and dopant diffusion in semiconductors is crucial for controlling the distribution of dopants during the fabrication of electronic devices. This is, in particular, important to meet the requirements for the continuing decrease of the lateral and vertical dimensions of semiconductor devices. Numerous diffusion experiments and spectroscopic studies have been conducted over the past few decades to determine the mechanisms of atomic-mass transport of self- and foreign atoms in elemental and compound semiconductors and the properties of point defects such as their structure, charge states, and formation and migration energies [1-3]. The advances in the understanding of atomic mass transport processes and defect reactions in semiconductors have contributed to the remarkable increase of computer speed and capacity over the last decades. The higher computer power gives rise to more reliable and predictive theoretical calculations of the properties of point defects in semiconductors and therewith expedites their own technological evolution.

A macroscopic approach of modelling the diffusion and reaction of point defects in materials are continuum-theoretical (CT) calculations based on differential equations. Within the

CT approach model parameters can be directly related to experimental profiles and a straight-forward interpretation of the diffusion process and the apparent diffusion coefficients can be given. Although the approach is more macroscopic compared to *ab-initio* and molecular dynamic (MD) simulations, the CT approach can provide information about the nature of the point defects, their charge states, and migration and formation enthalpies. A comparison with more microscopic simulations yields insight into the most likely atomic structure and migration path of the defect.

A powerful approach to investigate the properties of native point defects and the mechanisms of dopant diffusion in semiconductors is the analysis of the simultaneous dopant and self-diffusion in isotopically controlled multilayer structures [4]. These studies not only provide a strict consistency check of our present understanding of atomic transport processes and reactions in semiconductors mainly used for present electronic applications but also yield highly valuable information about the properties of point defects in semiconductors for future technological applications. Recent dopant diffusion experiments with isotopically controlled silicon isotope multilayer structure helped to determine the charge states and energy levels of native point defects in Si and demonstrate the power of this diffusion method [5, 6].

At present, a renewed interest in germanium both in its pure form and in combination with silicon exists for future commercial fabrication of field effect transistors [7]. This trend is mainly driven by the higher carrier mobility in germanium compared to silicon. In the past, material issues associated with the formation of insulating layers has hampered the application of germanium. However, recent developments in high-k dielectric materials have eliminated the former obstacles. Phosphorus, arsenic, and antimony are important n-type dopants for Ge-based technology. Their diffusion under intrinsic and extrinsic doping and their interaction with native point defects is discussed in this work. In order to control the enhanced dopant diffusion under extrinsic doping conditions, which is highly unfavorably for the fabrication of shallow junctions, defect engineering with carbon is proposed. Carbon in Ge can effectively reduce the enhanced diffusion of n-type dopants under extrinsic conditions via the formation of carbon-vacancy-dopant complexes. The results of this work form the basis for understanding dopant-defect interactions in Ge that help to control dopant diffusion according to the requirements for nanodevice fabrication.

## 2 Simultaneous Self- and Dopant Diffusion in Silicon

Isotopically controlled silicon heterostructures are well suited to investigate the impact of dopant diffusion on silicon self-diffusion. For these experiments we used isotope multilayer structures consisting of five alternating pairs of ^{28}Si/^{nat}Si that allow the measurement of depth-dependent self-diffusion that results from the diffusion of a dopant into the isotope structure. The dopants were introduced via implantation into an amorphous Si cap layer, thereby preventing any implantation damage from altering the equilibrium native defect concentrations in the isotope structure. The incorporation of dopants to concentrations that exceed the intrinsic carrier concentrations makes the material electronically extrinsic. As a consequence, the position of the Fermi level shifts, leading to a change in the thermal equilibrium concentration of charged native defects [8].

The diffusion of the dopants B, As, and P in Si stable isotope structures were investigated to determine the native defects and defect charge states responsible for diffusion in Si under extrinsic p-(B) and n-type (As, P) conditions [6]. Fig. 1 (a) and (b) show typical B and As diffusion profiles and the corresponding Si profiles obtained after diffusion annealing at 1000 °C and 995 °C, respectively. Various charged states of self-interstitials and vacancies were considered for modeling the experimental profiles [6]. Fig. 2 shows the ionization levels
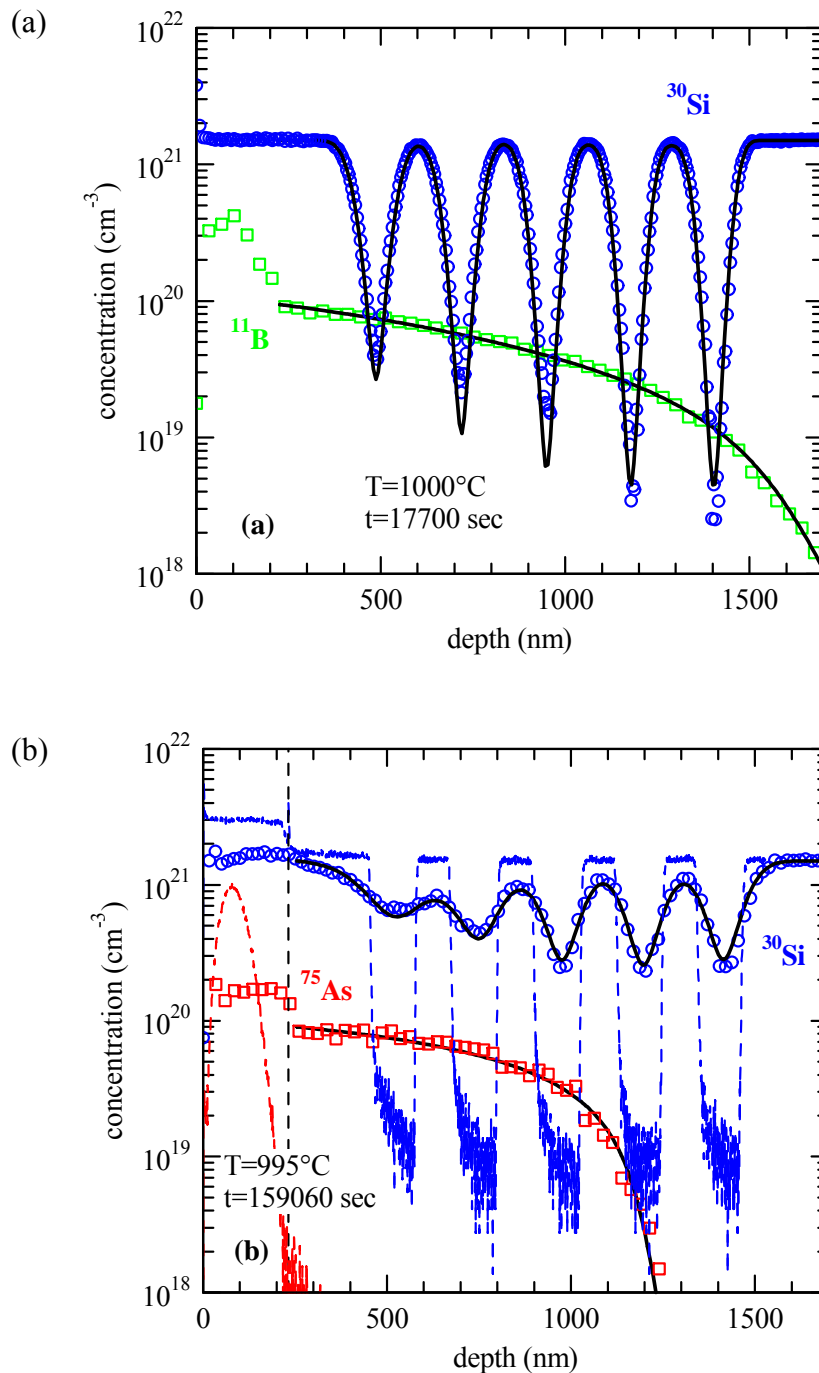
Fig. 1: SIMS concentration profiles of (a) boron (□) and (b) arsenic (□) and the corresponding silicon profiles (○) after annealing the silicon isotope multilayer structure at the temperatures and times indicated. The dopants were introduced by implantation into a top amorphous Si layer. The SIMS analyzes of the arsenic-implanted Si isotope structure is shown by the dashed lines in (b). The interface between the amorphous cap layer and the single crystalline Si structure is indicated by the vertical dashed line in (b). The solid lines represent numerical simulations on the basis of appropriate diffusion mechanisms that are discussed in detail in ref. [6].

of vacancies and self-interstitials in the Si band gap determined from the simultaneous diffusion of self- and dopant atoms as function of the inverse temperature. The comprehensive analysis reveals that neutral and negatively charged vacancies and neutral and positively charged self-interstitials mainly mediate the diffusion of P, As, and B in silicon [6].
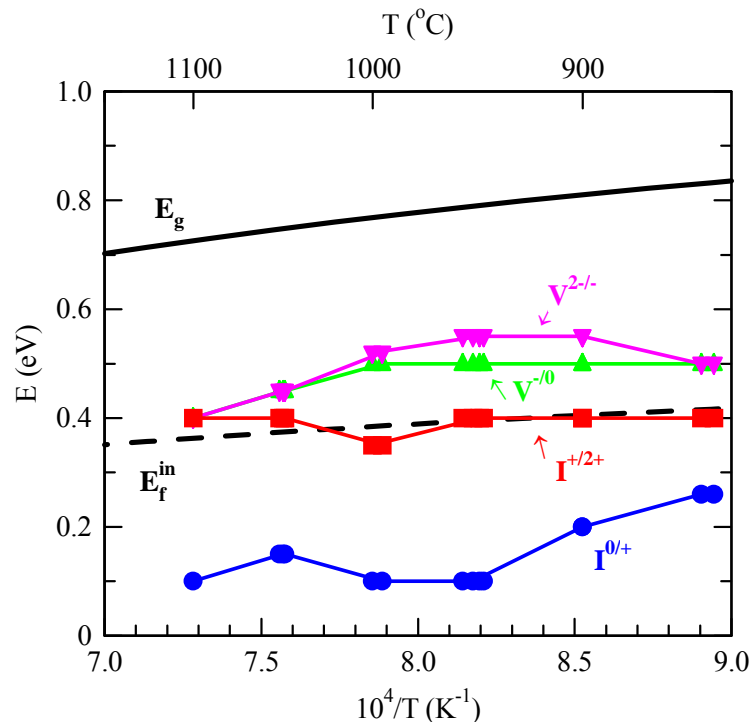
Fig. 2: Energy level positions of vacancies V and self-interstitials I within the band gap of Si for temperatures between 850 °C and 1100 °C. The temperature dependence of the Si band gap E_g and the Fermi level under intrinsic conditions E_f^{in} were calculated with the expressions given by Thurmond [9]. The symbols show the results from modeling the simultaneous self- and dopant diffusion. The thin solid lines are guides for the eye.

3 Dopant Diffusion in Germanium

Results on dopant diffusion in Ge date back forty to fifty years and are mainly based on p/n-junction and sheet resistance measurements [1]. More recent experiments on P [10, 11] and As [12] diffusion seem to be at variance with the former results. This inconsistency led us to perform experiments on intrinsic and extrinsic diffusion of the technologically most important n-type dopants P, As, and Sb in natural Ge. Compared to Si where the n-type dopants diffuse by means of self-interstitials and vacancies, the diffusion behavior in Ge is accurately described solely on the basis of the vacancy mechanism [13, 14]. Fig. 3 shows As diffusion profiles in Ge for intrinsic and extrinsic doping conditions. The intrinsic profile resembles a complementary error function with a constant diffusion coefficient. The extrinsic diffusion profile is box-shaped and reflects an apparent dopant diffusion coefficient that is proportional to the square of the dopant concentration [13, 14]. Both As profiles were obtained after diffusion annealing at the same temperature and time and clearly demonstrate the enhanced As diffusion under extrinsic conditions. The different doping levels were adjusted by changing the As partial pressure in the diffusion ampoule [14]. Additional profiles of As and of the n-type dopants P and Sb will be published elsewhere [14]. Accurate modeling of the intrinsic and extrinsic diffusion is achieved on the basis of the vacancy mechanism [13, 14]

$$AV^- \rightleftharpoons A_S^+ + V^{2-} \tag{1}$$

Here A denotes P, As, or Sb. AV^- and A_S^+ are the singly negatively charged dopant-vacancy pair and the singly positively charged substitutional donor, respectively. The charge state of

the vacancy V is considered to be doubly negative. This is at variance with the self-diffusion study of Werner et al. [15], who suggested that vacancies in Ge are neutral and singly negatively charged. Evidence of the charge of the vacancies results from the experiments on the simultaneous diffusion of self- and dopant atoms in Ge isotope multilayer structures (see below). Detailed analysis of intrinsic and extrinsic dopant diffusion in Ge yields that the apparent diffusion coefficient D_A of the dopant A at a particular doping level n (n = free electron concentration) is given by [13, 14]

$$D_A(n) = D_A(n_i) \left(n/n_i \right)^2. \tag{2}$$

$D_A(n_i)$ is the dopant diffusion coefficient under intrinsic conditions and n_i the intrinsic carrier concentration. The temperature dependence of dopant diffusion under intrinsic conditions is accurately described with an Arrhenius equation. The activation enthalpies and pre-exponential factors were determined to 2.85 eV and 9.1 cm^{2}s^{-1} for P, 2.71 eV and 32 cm^{2}s^{-1} for As, and 2.55 eV and 16.7 cm^{2}s^{-1} for Sb [14]. The values obtained for n_i are in good agreement with the data reported by Morin and Maita [16]. It is noticeable that the diffusion activation enthalpies decrease with increasing atomic size of the dopant element. This characteristic is attributed to differences in the binding energy of the dopant-vacancy pairs.

To investigate the interference between self- and dopant diffusion we also performed experiments with isotopically enriched Ge multilayer structures. Thermal annealing of the isotope structure without indiffusion of the dopants leads to a homogeneous intermixing [17] that is accurately described with the Ge self-diffusion data reported by Werner et al. [15]. This demonstrates that the epitaxial structure grown by molecular beam epitaxy (MBE) is well suited for diffusion studies. Diffusion of the n-type dopants into the isotope structure proceeds from an arsenic implanted amorphous Ge cap layer and from infinite GeAs, GeP or GeSb
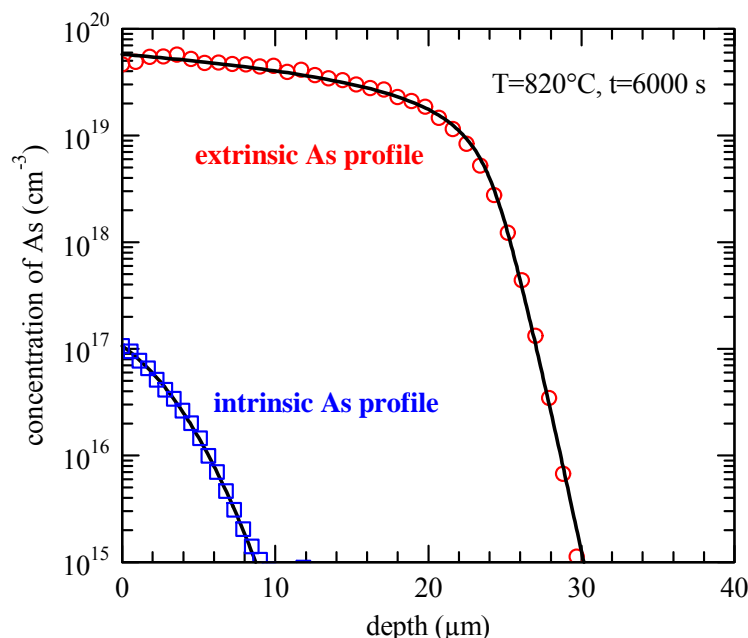
Fig. 3: Concentration profiles of substitutional As measured by means of the spreading resistance technique after diffusion annealing at 820°C for 6000 s. The lower (□) and upper (○) As profiles reflect the diffusion behaviour under intrinsic and extrinsic doping conditions, respectively. The profiles illustrate the enhanced As diffusion under extrinsic doping conditions. The As diffusion behaviour is accurately described on the basis of reaction (1) (solid lines) (for details see refs. [13, 14]). For clarity only a reduced number of data points are shown.

alloy sources that were encapsulated in closed silica ampoules together with the Ge samples. For comparison both natural and isotopically enriched samples were annealed simultaneously. Dopant and self-atom profiles measured with SIMS after annealing are illustrated in Fig. 4.

The SIMS analysis reveals an enhanced intermixing of the ^{nat}Ge/^{70}Ge layers within the dopant profiles indicating that the native defect mediating Ge self-diffusion must be negatively charged. Moreover, the SIMS analysis exhibits a peculiar step-up of the dopants within the originally ^{70}Ge layers whereas the dopant profile in natural Ge shows the expected box shape. With the dopant step-up also the dopant penetration depth is reduced in the Ge isotope structure. The apparent dopant segregation in the isotope structure and simultaneous slow-down of the dopant diffusivity are characteristic for a trap-limited diffusion [18]. The step-up of the dopant concentration is located within the original ^{70}Ge layers and is not affected by the intermixing of the ^{nat}Ge/^{70}Ge layers. This indicates that an immobile defect must be present within the ^{70}Ge layers to concentrations similar to the doping level. Additional SIMS measurements revealed that carbon has been unintentionally introduced during the MBE growth of the ^{70}Ge layers to concentrations close to 10^{20} cm^{-3}. This exceeds the solubility of carbon in Ge by several orders of magnitude [19]. The carbon distribution in the isotope structure is not affected by annealing, *i.e.*, the annealed sample shows a carbon distribution identical to that of the asgrown structure. Transmission electron microscopy of the asgrown and annealed isotope structures did not show any carbon precipitates within the ^{70}Ge layers. Presumably carbon is mainly incorporated on substitutional site during the MBE growth of the structure. It is also noticeable that the shape of the dopant profile is less box-shaped in the case when the dopant concentration is close to 10^{20} cm^{-3}. This becomes evident by the P profile in the natural and isotopically enriched Ge samples (see Fig. 4). In the first case the expected box-shaped P profile is obtained for a maximum doping level of about 3×10^{19} cm^{-3} whereas the latter sample
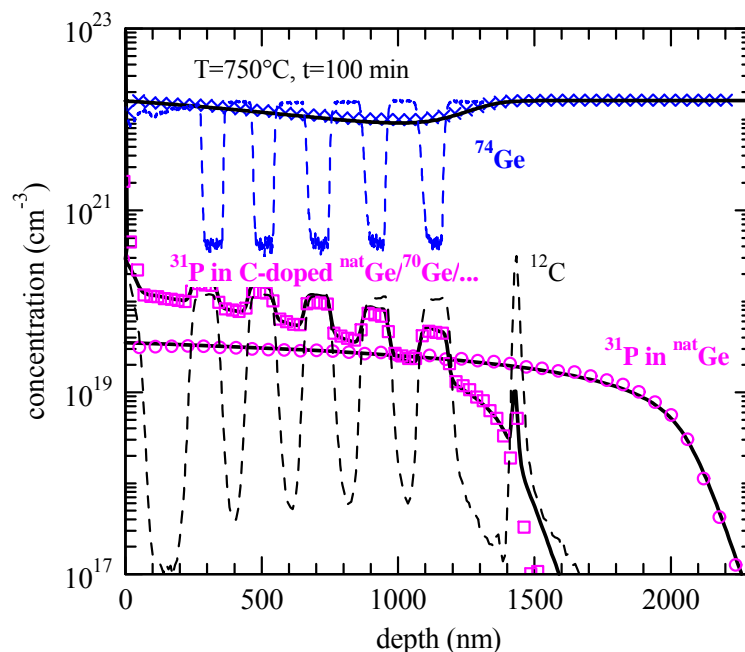
Fig. 4: SIMS concentration profiles of P in natural Ge (○) and isotopically controlled Ge multilayer structures (□) measured after diffusion annealing at 750°C for 100 min. The corresponding ^{74}Ge profile (×) is compared to the asgrown structure (upper dashed line). The enhanced P concentration within the enriched ^{70}Ge layers is due to trapping of P by carbon whose distribution after annealing is shown by the lower dashed line. The trapping of P leads to a reduced P diffusivity as demonstrated by the lower P penetration depth in the ^{nat}Ge/^{70}Ge multilayer structure compared to the ^{nat}Ge sample. The solid lines are best fits on the basis of reactions (1), (3) and (4).

reveals a far less pronounced box-shaped P profile for concentrations close to 10^{20} cm^{-3}. This observation is at variance with the diffusion behavior of n-type dopants in Ge expected on the basis of eqn. (1) [14]. In order to accurately account for the trapping of n-type dopants within the carbon-doped ^{70}Ge layers and the change in the shape of the dopant profiles for high dopant concentrations the following reactions are assumed in addition to eqn. (1)

$$AV^- + \ C^0 \rightleftharpoons (CVA)^0 + e^- \tag{3}$$

$$AV^- + A_S^+ \rightleftharpoons (A_2V)^0 \tag{4}$$

eqn. (3) accounts for the trapping of mobile AV^- pairs within the C-doped ^{70}Ge layers. eqn. (4) describes the formation of neutral dopant-vacancy complexes $(A_2V)^0$. The charge states assigned to the various defects follow from the demand to accurately describe both the dopant and self-atom profiles. Best fits to the experimental profiles are illustrated by the solid lines in Fig. 4. The quality of the fit demonstrates that simulations on the basis of reactions (1), (3), and (4) accurately describe the diffusion behavior of the n-type dopants in natural high purity Ge and the simultaneous self- and dopant diffusion in carbon doped Ge isotope heterostructures. It is noted that the experimental profiles are unique with respect to the charge states of the vacancy, the carbon trapping center, the carbon-dopant complex, and the dopant complex in reaction (4). However, the nature of these defects can not be determined unambiguously. But the defects assumed in reactions (3) and (4) are the most straightforward defects whose formation is supported by the recent ab-initio calculations of Chroneos et al. [20, 21].

4 Conclusions

Dopant diffusion in isotope heterostructures is a powerful approach for studying diffusion and defect reactions in semiconductors. Recent diffusion studies with isotopically controlled silicon heterostructures provide the charge states and energy level positions of self-interstitials and vacancies in Si [5, 6]. Utilizing natural and isotopically enriched Ge multilayer structures the diffusion of the n-type dopants P, As, and Sb was found to be mediated by singly negatively charged dopant-vacancy pairs and the Ge self-diffusion by doubly negatively charged vacancies. Doping the ^{70}Ge layers of the ^{nat}Ge/^{70}Ge isotope structure with carbon leads to trapping of the dopant within the C-doped layer and a retarded dopant diffusion. The formation of neutral dopant-vacancy complexes becomes evident from the change in the dopant profile at high dopant concentrations. The type of the defects assumed in eqns. (1), (3), and (4) is confirmed by ab-initio calculations [20, 21]. These calculations predict the stability of CVA [20] and A$_n$V (with $n = 1, 2, 3, 4$) complexes [21] in Ge. The impact of carbon on n-type dopant diffusion in germanium described in this work may help to control the enhanced dopant diffusion under extrinsic doping conditions which is proportional to the electron concentration squared (see eqn. (2)).

References

[1] Diffusion in Semiconductors and Non-Metallic Solids, edited by D.L. Beke, Landolt-Börnstein, New Series, Group III, Vol. 33A (Springer, Berlin, 1998).

[2] Impurities and Defects in Group IV Elements, IV-IV and III-V Compounds, edited by M. Schulz, Landolt-Börnstein, New Series, Group III, Vol. 41A2, Part α (Springer, Berlin, 2002).

[3] Impurities and Defects in Group IV Elements, IV-IV and III-V Compounds, edited by M. Schulz, Landolt-Börnstein, New Series, Group III, Vol. 41A2, Part β (Springer, Berlin, 2003).

[4] H. Bracht, H.H. Silvestri, and E.E. Haller, Solid State Commun. 133 (2005) 727-735.

[5] H. Bracht, Phys. Rev. B 75 (2007) 035210-1(16).

[6] H. Bracht, H.H. Silvestri, I.D. Sharp, and E.E. Haller, Phys. Rev. B 75 (2007) 035211-1(21).

[7] Cor Claeys and Eddy Simoen (Eds), Germanium-based Technologies - From Materials to Devices, (Elsevier, Amsterdam, 2007).

[8] W. Shockley and J.T. Last, Phys. Rev. 107 (1957) 392.

[9] C.D. Thurmond, J. Electrochem. Soc. 122 (1975) 1133.

[10] Chi On Chui, K. Gopalakrishnan, P.B. Griffin, J.D. Plummer, and K.C. Saraswat, Appl. Phys. Lett. 83 (2003) 3275.

[11] M.S. Carroll and R. Koudelka, Semicond. Sci. Technol. 22 (2007) S164.

[12] E. Vainonen-Ahlgren, T. Ahlgren, J. Likonen, S. Lehto, J. Keinonen, W. Li, and J. Haapamaa, Appl. Phys. Lett. 77 (2000) 690.

[13] H. Bracht and S. Brotzmann, Materials Science in Semiconductor Processing 9 (2006) 471.

[14] S. Brotzmann and H. Bracht, J. Appl. Phys. 103 (2008) 033508.

[15] M. Werner, H. Mehrer, and H.D. Hochheimer, Phys. Rev. B 32 (1985) 3930.

[16] F.J. Morin and J.P. Maita, Phys. Rev. 94 (1954) 1525.

[17] S. Schneider, H. Bracht, M.C. Petersen, J. Lundsgaard Hansen, and A. Nylandsted Larsen, J. Appl. Phys. 103 (2008) 033517.

[18] A. Rodriguez, H. Bracht, and I. Yonenaga, J. Appl. Phys. 95 (2004) 7841-7849.

[19] E.E. Haller, W.L. Hansen, P. Luke, R. McMurray, and B. Jarrett, IEEE Transactions on Nuclear Science, 29 (1982) 745-750.

[20] A. Chroneos, B.P. Uberuaga, and R.W. Grimes, J. Appl. Phys. 102 (2007) 083707.

[21] A. Chroneos, R.W. Grimes, B.P. Uberuaga, S. Brotzmann, and H. Bracht, Appl. Phys. Lett. 91 (2007) 192106.